ELSEVIER

# Influence of a glacial buzzsaw on the height and morphology of the Cascade Range in central Washington State, USA

Sara Gran Mitchell \*, David R. Montgomery

*Department of Earth and Space Sciences, University of Washington, Box 351310 Seattle, Washington 98195, USA*

## Abstract

Analysis of climatic and topographic evidence from the Cascade Range of Washington State indicates that glacial erosion limits the height and controls the morphology of this range. Glacial erosion linked to long-term spatial gradients in the ELA created a tilted, planar zone of 373 cirques across the central part of the range; peaks and ridges now rise ≤600 m above this zone. Hypsometric analysis of the region shows that the proportion of land area above the cirques drops sharply, and mean slopes >30° indicate that the areas above the cirques may be at or near threshold steepness. The mean plus 1σ relief of individual cirque basins (570 m) corresponds to the ∼600-m envelope above which peaks rarely rise. The summit altitudes are set by a combination of higher rates of glacial and paraglacial erosion above the ELA and enhanced hillslope processes due to the creation of steep topography. On the high-precipitation western flank of the Cascades, the dominance of glacial and hillslope erosion at altitudes at and above the ELA may explain the lack of a correspondence between stream-power erosion models and measured exhumation rates from apatite (U-Th/He) thermochronometry.
© 2005 University of Washington. All rights reserved.

*Keywords:* Glacial erosion; Topography; Digital elevation model analysis; Cascade Range; Washington State

## Introduction

The complex relationships among climate, tectonics, erosion, and topography in the world's mountain ranges encompass issues of substantial ongoing interest in geomorphology (Burbank et al., 1996; Montgomery et al., 2001; Whipple et al., 1999). Relatively new topographic analysis techniques using digital elevation models (Brocklehurst and Whipple, 2004; Montgomery et al., 2001), the recent application of low-temperature thermochronometry methods such as apatite (U-Th)/He dating (e.g., House et al., 1997; Reiners et al., 2002), and the development of new landscape evolution models (MacGregor et al., 2000; Tomkin and Braun, 2002) allow the investigation of these relationships in glaciated terrain. Here, we explore linkages between climate and topography as set by the physical effects of long-term glacial erosion on the height and morphology of the Cascade Range in central Washington State.

The correspondence of glacier snowline altitudes to the maximum elevation of mountain ranges has been recognized for over a century (Mills, 1892), although whether such a relationship is governed by topographic controls on snowline altitude or erosional controls on topography has remained unsettled. Several recent studies have shown that glacial erosion can dominate the topographic form of mountain ranges that rise high enough to intersect the local glacier equilibrium-line altitude (ELA). Brozovic et al. (1997) showed that mean altitude, hypsometry, and slope distributions in the Himalaya correlate with the snowline, independent of large gradients in the modern uplift rate deduced from thermochronometry. Whipple et al. (1999) subsequently suggested that glaciers reduce mountain range relief by focusing glacial erosion at and above the ELA, decreasing fluvial erosion downstream from glaciers in sediment-choked valleys, and enhancing periglacial erosion on high peaks. Montgomery et al. (2001) showed a correlation between the ELA and peak altitudes in the Andes. Brocklehurst and Whipple (2002) suggested that in the eastern Sierra Nevada, glaciers concentrate overall mass removal to altitudes above the regional ELA, thus reducing overall relief. Spotila et al.

---

\* Corresponding author. Fax: +1 206 543 0489.
 *E-mail address:* sgm1@u.washington.edu (S.G. Mitchell).

(2004) used apatite (U-Th)/He thermochronometry (AHe dating) to show that denudation patterns in the Chugach-St. Elias Range of Alaska correlate with the distribution of glaciers and that erosion rates are sufficiently high to remove rock as it is uplifted due to tectonic convergence. These studies have produced an intriguing hypothesis regarding a "glacial buzzsaw" effect: that glacial erosion can rapidly denude topography raised above the ELA, regardless of rock uplift rate or lithology, and thereby limit how high mountains may rise.

Despite evidence for such an effect, key questions remain. Can we define specific topographic characteristics of a glacial buzzsaw, or determine through what physical processes does the buzzsaw operate? Are such processes common to all glaciated mountain ranges? Glacial erosion has been shown to sculpt landscapes into distinctive forms and is thought to be relatively rapid (e.g., James, 2003; Hallet et al., 1996). For example, repeated alpine glaciation increased the size and relief of valleys since the start of the Pleistocene in both the Olympic Mountains of Washington State (Montgomery, 2002) and in central Idaho (Amerson, 2005). Paraglacial processes, defined by Ballantyne (2002) as the "nonglacial earth−surface processes... directly conditioned by glaciation and deglaciation," may also enhance erosion rates through the creation of unstable or metastable landscapes upon deglaciation. We propose that in the Cascades, alpine glaciation scours out threshold hillslopes selectively at and above a zone of cirques formed at or close to the Quaternary average ELA. This enhanced erosion effectively creates a limiting envelope of peak and ridge heights tied to the ELA rather than modern fluvial processes or spatial gradients in long-term exhumation. We test this hypothesis using morphometric and thermochronologic techniques to investigate the relationship between topography, climate, geology, erosion rates, and the altitude of modern glaciers and glacial landforms.

## Study area and previous work

The portion of the Cascade Range located in central Washington is an ideal setting in which to investigate the relationship between glacial activity and topography (Fig. 1). First, the topography and geology have been mapped in detail. Spatial data for this region include topography from 10-m grid-size digital elevation models (DEMs) constructed from USGS quadrangles (Fig. 2A), and digital geologic maps at 1:100,000 scale (Fig. 2B). Second, the N−S-trending range crest is perpendicular to a strong, west−east precipitation gradient caused by the orographic disruption of the eastern trajectory of weather systems originating in the Pacific Ocean. Precipitation data obtained from the Spatial Climate Analysis Service, Oregon State University (http://www.ocs.orst.edu/prism) show that the modern average annual precipitation ranges from >4 m yr$^{-1}$ in the central part of the study area to <1 m yr$^{-1}$ at the far eastern edge of the range (Fig. 2C). This precipitation gradient creates distinct spatial gradients in both fluvial erosion potential and the ELA (Porter, 1964; Roe et al., 2002). Third, previous studies in the Cascades provide us with ~90 low-temperature thermochronometry ages with which to investigate the relationship between long-term exhumation and topography (Reiners et al., 2002, 2003).

The Cascades in Washington were extensively glaciated during the Pleistocene. The glacial geology and glacial limits of major Cascade valleys have been mapped, and the trends in modern and Pleistocene ELAs are known for much of the Cascades (e.g., Porter, 1964, 1976a, 1989). We restricted our investigation to an area south of where the Cordilleran Ice Sheet covered high topography, an area of mountainous terrain sculpted predominantly by alpine and valley glaciers (Long, 1951; Mackin, 1941; Page, 1939; Waitt, 1975; Waitt and Thorson, 1983; Booth et al., 2004). A small part of the Puget Lowland, an area once covered by the Puget Lobe of the Cordilleran Ice Sheet, is included in the far western part of our study area; however, our analyses focus on the higher topography to the east.

This study builds upon previous physiographic investigations in the Cascade Range, including the early studies of Russell (1900), Willis (1903) and Smith (1903). Russell and Willis both noted that non-volcanic peaks and ridges in the Cascades rise to about the same altitude across the range, suggesting that the peaks were remnants of an uplifted and incised erosion surface. The remains of some relatively low-relief, high-altitude, tilted surfaces suggestive of an uplifted low-relief landscape are preserved on the eastern flank of the Cascades (Porter, 1976b). Smith (1903) acknowledged the uplifted peneplain theory, but argued that on the west side of the range, higher rates of precipitation had so dissected the terrain that the peaks today stand an unknown distance lower than the original surface, and that slow, spatially complex uplift probably means that a table-like plateau never existed. Alternatively, Daly (1905) suggested that concordance of the peaks was a function of treeline because erosion rates should be relatively high in the exposed areas above treeline due to
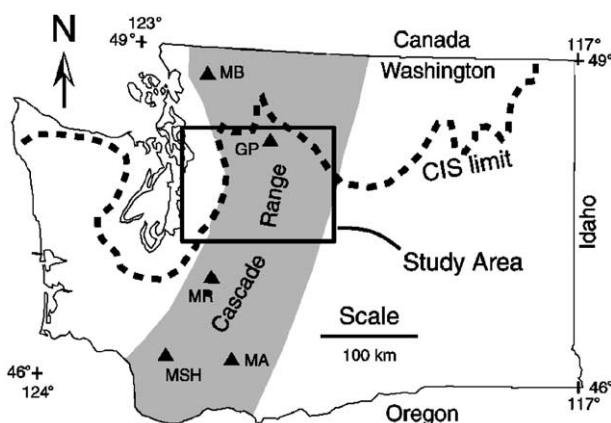


Figure 1. Location of study region. The area of the Washington Cascades is shaded in gray, with the study area marked by the box. Quaternary Cascade volcanoes are marked with triangles (MB = Mt. Baker, GP = Glacier Peak, MR = Mount Rainier, MSH = Mt. St. Helens, MA = Mt. Adams). Southern limit of the Cordilleran Ice Sheet (CIS) shown as heavy dashed line (Booth et al., 2004).
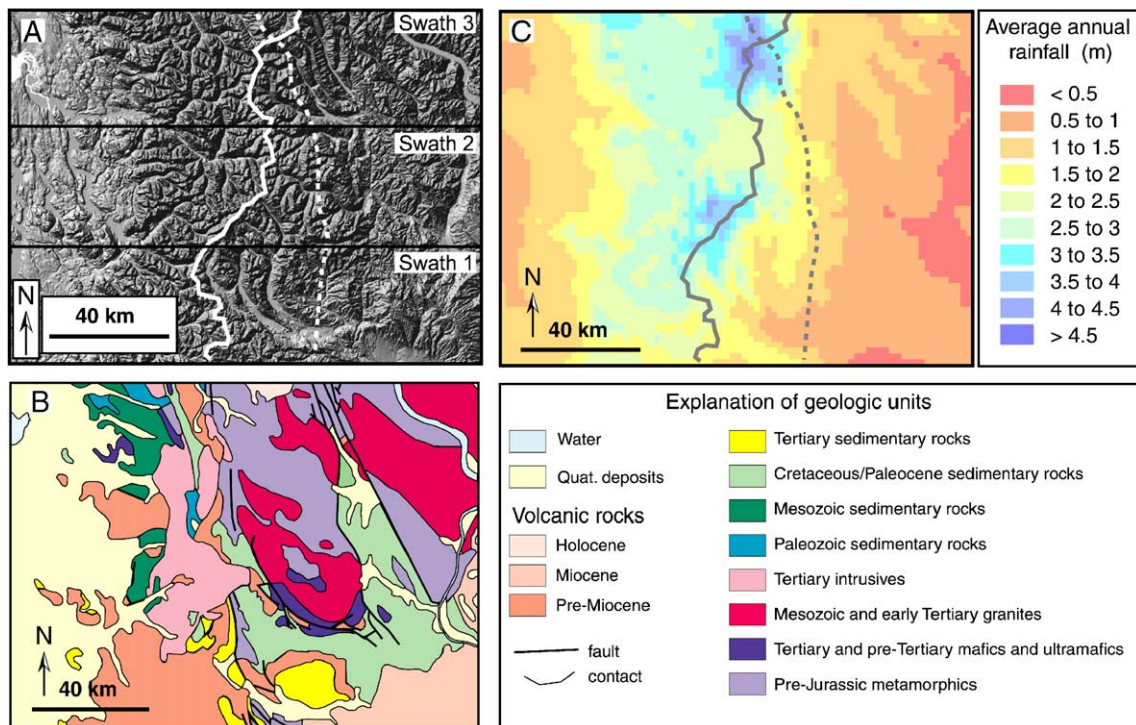
Figure 2. (A) Shaded relief map of study area. Black horizontal lines delineate swaths 1, 2, and 3. Solid white line shows the position of the drainage divide, white dashed line shows the approximate position of the range crest. (B) Generalized geology modified from Weissenborn (1969). (C) Average annual precipitation (1960–1991) over the study area, in meters. The drainage divide and range crest are shown as gray solid and dotted lines, respectively. Precipitation data come from the Spatial Climate Analysis Service (Oregon State University, http://www.ocs.orst.edu/prism).

the lack of protective effects of trees and their roots. The treeline hypothesis was later embraced by Thompson (1962), who suggested that increased rates of mass wasting above treeline are evident over much of the high alpine regions of the western United States, including the Cascades Range in Washington.

More recently, the relationship between large-scale trends in altitude and the extent of past and present glaciations has been the subject of investigations in the Cascades. ELAs of modern glaciers are significantly higher on the eastern flank of the Cascades than on the western flank (Porter, 1977, 1989). Porter (1977) examined cross-range trends in glacier altitude, by investigating trends in a "glaciation threshold," defined as the average altitude of the lowest glacier-bearing peak and the highest nonglaciated peak within a USGS 7.5-min topographic quadrangle. This method avoids the problem of small-scale variability in individual mean glacier altitudes resulting from differences in slope and basin topography. However, this approach dictates that the glaciation threshold is inherently a function of nearby peak altitudes. This glaciation threshold increases in altitude to the east at a rate of about 12 m/km due to a strong W–E gradient in accumulation season precipitation (Porter, 1977). When considered as a group, the individual ELAs of existing glaciers and those of the last glacial maximum have also been found to rise eastward at about the same rate. In addition, a zone of cirques lies parallel to and between modern and last glacial maximum ELAs (Porter, 1989). Porter (1989) hypothesized that this zone of cirques defines the altitude range

where active, eroding glaciers spent the most time during the Quaternary, and thus represents a Quaternary average position of the ELA.

In addition, a considerable amount of low-temperature thermochronometric data has been collected for the Cascades (Reiners et al., 2002, 2003). Exhumation data from our study area indicate that there have been strong gradients in rock uplift across the range during the Cenozoic. These data indicate a pulse of rapid rock uplift and exhumation in the Cascades occurred during the late Miocene, and that precipitation is a dominant control on the spatial pattern of exhumation rates (Reiners et al., 2002, 2003).

## Methods

We apply a combination of spatial and topographic analyses to investigate the relationships between the extent of glaciation, geology, and the morphometry of our study area. We use GIS to: (1) characterize the "surface" created by the maximum topography of peaks and ridges, (2) apply three different erosion models to the topography to compare with measured exhumation rates, (3) create digital maps of modern glaciers and cirques to determine spatial trends in the ELA, (4) analyze the hypsometry and slope distributions of the region, and (5) investigate the altitude, relief, slope, and lithology of cirque basins. We also employ the data of Reiners et al. (2002, 2003), along with topographic analysis and erosion models to investigate the influence of glacial erosion on the central Washington Cascades.

*Maximum topography and hypsometry*

We use the DEM to characterize the "peak concordance" or surface formed by the peaks and ridges in the study area. We generalize cross-range trends in altitude with W–E oriented minimum, maximum, and mean altitude profiles constructed at 10-m intervals across the analysis window. Because of N–S variations in altitude, we subdivide the study area into three west-to-east profiles.

To test the suggestion that glaciated regions have area–altitude relationships that correlate with the extent of glaciation or snowline altitude (e.g., Brocklehurst and Whipple, 2004; Brozovic et al., 1997), we generate hypsometric curves for the study area. These hypsometric curves indicate the amount of land surface area within defined altitude intervals. Because the topography of the study region has such a strong W–E trend, we divide the DEM into eight N–S-oriented, 20-km-wide swaths that range from west to east across the region. Within each swath, we then measure the area within 100-m altitude bins.

*Exhumation rates and erosion indices*

Because we are interested in the relative effects of glacial erosion on the Cascades, we must also consider the potential influence of fluvial and hillslope erosion processes. If long-term fluvial erosion and rock uplift have been the primary controls on the morphology of the Cascades, we would expect to see a relationship between fluvial erosion models, such as stream power or unit stream power and long-term exhumation, with high exhumation rates near channels of high discharge and slope. Similarly, if hillslope erosion drives the topography of the range, high measured exhumation rates should be found in the regions of steep slopes and high precipitation. To test these potential relationships, we generate a fluvial erosion index based on stream power, and create a hillslope erosion index for the region based on slope and precipitation to compare with exhumation patterns.

We calculate stream power using the standard equation from Bagnold (1960), quantifying the energy expenditure per unit channel length:

$$\Omega = \rho g Q S \qquad (1)$$

where $\Omega$ is stream power, $\rho$ is the density of water (1000 g m$^{-3}$), g is acceleration due to gravity (9.81 m s$^{-2}$), and slope (S) is a unitless parameter defining the steepest descent between each cell and any of its neighbors. Instead of making the conventional substitution of drainage area for discharge (Q), we calculate discharge (m$^3$ s$^{-1}$) for each cell by calculating a precipitation-weighted flow accumulation using annual precipitation data from 1960 to 1990, obtained from the Spatial Climate Analysis Service at Oregon State University (http://www.ocs.orsu.edu/prism) and a flow network generated using GIS. This discharge calculation assumes all precipitation falling on a region becomes runoff, ignoring factors such as infiltration, evaporation, and transpiration. Hence, as discussed by Finlayson and Montgomery (2003), discharges estimated by these methods need to be calibrated to represent discharges of a particular recurrence interval or frequency. Because erosion rate is proportional to bedrock erodibility, we modeled stream power to simply indicate spatial differences in erosion potential, rather than as a measure of erosion rate (Finlayson and Montgomery, 2003).

Hillslope erosion potential is calculated simply as the product of mean annual precipitation and slope. All else being equal, regions with steep slopes and high rainfall should prove more vulnerable to most hillslope processes, including discrete events such as deep-seated landslides, debris flows, as well as less-catastrophic processes such as rainsplash and creep. The potential for erosion rate to increase non-linearly on steep hillslopes (e.g., Martin, 2000; Martin and Church, 1997; Montgomery and Brandon, 2002; Roering et al., 1999) would tend to reduce any such correlation for threshold slopes.

We examine the relationship between the fluvial and hillslope erosion models with measured long-term exhumation rates. Hypothesizing that if either fluvial or hillslope erosion drives topographic development in the Cascades, and assuming a relatively low variability in bedrock erodibility across the range, we should see high exhumation in regions of high erosion potential. To test this idea, we identify the maximum fluvial and average hillslope erosion potential within a 5-km radius from each sample site for (U-Th)/He exhumation rates (Reiners et al., 2003) and plot these indices against the measured exhumation rates. The 5-km radius was chosen to approximate the average valley width; this length radius assures capturing a channel in the same basin as the sample location for the maximum fluvial erosion index measurement, and it integrates a large enough portion of the landscape to avoid local effects for the hillslope erosion index. To understand the dominant geomorphic influences on exhumation, we subdivide the sample localities based on several additional parameters, including location relative to the range crest (east or west), annual precipitation, and sample elevation. Finally, we investigate the relationship between the long-term exhumation and the location and character of the maximum topographic envelope defined by the peak altitudes.

Glacial erosion is considerably more complex than fluvial erosion, and we have not attempted to model it here. However, in general, landscape evolution models incorporating glacial erosion show that it is concentrated at altitudes at and above the ELA (e.g., Tomkin and Braun, 2002; MacGregor et al., 2000). This glacial erosion can also influence rates of fluvial erosion downstream and can act to reduce relief on a basin-wide scale (e.g., Whipple et al., 1999). Glacial erosion, largely a function of basal ice sliding velocity, scales non-linearly with precipitation, slope, and accumulation area (e.g., Tomkin and Braun, 2002). Thus, in areas where glacial erosion dominates, long-term patterns in exhumation may not correlate spatially with fluvial processes. Conversely, we may expect to see similarities between glacial and hillslope erosion patterns, as both scale similarly with precipitation.

*Topographic trends of glaciers and cirques*

We use the mean altitudes of modern glaciers to determine the trend in the modern ELA across the study area (Charles-

worth, 1957). Glacier locations are derived from areas >1 km² mapped as permanent ice on the 60-min, 1:100,000-scale digital geologic maps of Washington State (Tabor et al., 1982, 1987, 1993, 2000), though we recognize that not all permanent ice constitutes an active glacier. These regions mapped as permanent ice are overlain on the topography of the study area and clipped to make individual DEMs of each presumed glacier. We use these individual DEMs to determine UTM coordinates of the centroid and calculate the median altitude of each glacier (Porter, 2001). Recognizing this measurement as a rough approximation (e.g., Benn and Lehmkuhl, 2000), we use this median altitude as a proxy for ELA.

Because the modern ELA represents the area of active glaciation for only a small part of the total glaciated interval, we follow the general methods of Porter (1989) and analyze the topography and geology of individual cirque basins in the study area to estimate the Quaternary average ELA. For our analysis of cirque basins, we first identify the cirques visually with digital raster graphics (DRGs) of USGS 7.5-min topographic maps. We select semi-circular-shaped basins with bowl-shaped depressions or a broad, flat area in the center (e.g., Rudberg, 1984). Many, but not all, of the cirques have a lake on the cirque floor (i.e., a tarn). Using the DRGs as a guide, we find the UTM coordinates and altitudes of the cirque drainage outlets. We use the altitudes of these drainage outlets to define the "minimum" cirque altitudes, regardless of whether or not the cirque is overdeepened, contains a tarn, or is filled with sediment.

We then use these basin outlets and a flow-direction algorithm run on the 10-m DEM to delimit the basin areas for individual cirques; these basin areas represent the contributing watershed area for each cirque outlet, including the adjacent peaks and ridges. We verified the accuracy of the automated basin-delimiting program by overlaying the cirque boundaries on the DRGs of each basin boundary. Because we are particularly interested in the relationships between the minimum altitudes for each cirque and the height of its surrounding peaks, we calculated the relief in each cirque basin by subtracting the altitude of the cirque outlet from the maximum altitude in each watershed. Because the outlet may not represent the lowest altitude of the cirque, the cirque relief so defined consequently is a minimum. Finally, we identified the bedrock underlying each cirque to determine if there are relationships between rock type and cirque basin relief. Bedrock geology was identified using the 1:100,000-scale digital geologic maps of Washington State and divided into the following broad categories: plutonic igneous, volcanic igneous, metamorphic, and sedimentary (including volcaniclastic deposits) (Tabor et al., 1982, 1987, 1993, 2000).

*Slope distributions*

We also analyze differences in the steepness of the cirque basins relative to the overall topography, as well as consider whether the topography is composed of threshold slopes that stand as steep as supportable for the local relief, drainage density, and rock type (e.g., Burbank et al., 1996; Montgomery,

2001; Schmidt and Montgomery, 1995). Slopes throughout the study area were calculated from the elevations of each DEM cell's eight nearest neighbors. We generated slope distributions by determining the number of cells within single-degree bins and analyzed the slope distributions for both the entire study area and for just the small fraction of topography contained within the cirque basins.

## Results

Excluding the Quaternary-aged volcanic cone of Glacier Peak, the maximum and mean altitudes in the study area systematically increase from west to east, with the maximum altitudes located 10 to 40 km east of the drainage divide. The high peaks on the western flank of the range define an inclined "surface" (Fig. 3). This inclined peak surface increases in altitude eastward at a gradient of 9 to 15 m km⁻¹ (Table 1). East of the range crest, the planar nature of the peak "concordance" loses its distinction.

Most of the glaciers present within the study area are concentrated in four main areas of relatively high topography: Glacier Peak, Mount Stewart, Alpine Lakes and Monte Cristo Peak (Fig. 4). Excluding the 16 glaciers located within 2.5 km of the volcanic Glacier Peak summit, mean glacier altitudes for the entire area average 1990 ± 240 m. Overall, glacier altitudes rise eastward at a linear gradient of ~11 m km⁻¹ (Table 1, Fig. 5). This gradient is slightly less steep in the far northern part of the range. The altitudes of the 373 cirque outlets identified in the study area follow a similar linear trend, with mean altitudes rising from west to east at ~13 m km⁻¹ (Table 1). These gradients in median glacier and cirque outlet altitudes are roughly parallel to the gradient in peak altitudes, which ranges from 9 to 15 m km⁻¹. The trend of the least-squares linear regression of cirque outlets is ~500 m lower than the corresponding regressions for the peaks and the modern glaciers.

Hypsometry of the area shows that in the far western portion of the study area (which includes significant amounts of the Puget Lowland) most of the land is at the low end of the altitude distribution. Not surprisingly, significantly more topography is found at higher altitude near the center of the range, where altitudes are more normally distributed (Fig. 6). The altitude–area distribution has a different shape in each of the eight swaths, and both mean and maximum altitude increase to a maximum near the center of the study area. However, one constant among the different regions is that in every swath that contains cirques, the amount of land surface area begins to drop off steeply at the altitude of the lowest cirques and a mere 4 to 14% of the land surface area exists above the highest cirque in each swath (Fig. 6).

The relief between the cirque outlets and the adjacent peaks or ridges ranges from 35 m to nearly 1200 m, averaging 380 ± 190 m (Fig. 7A). Only 10% of cirque basins have >600 m of relief. Cirque relief does not appear to be controlled by lithology. Relief in cirques underlain predominantly by plutonic (N = 219), volcanic (N = 27), metamorphic (N =
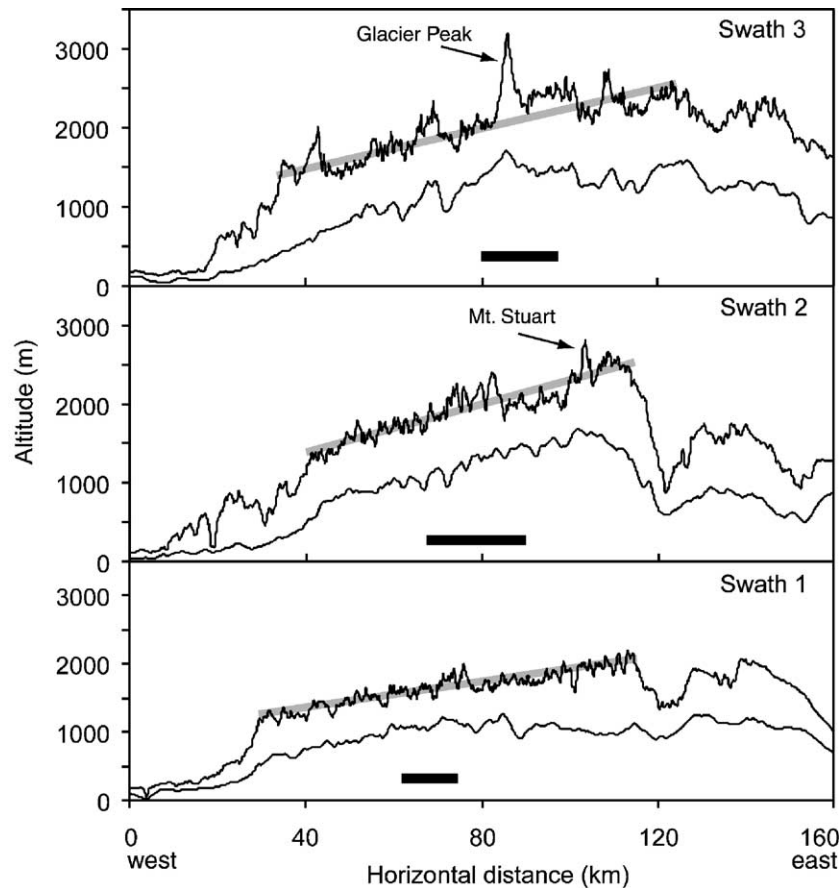
Figure 3. West-east topographic profiles of mean and maximum altitudes for swaths 1, 2, and 3. Linear regressions of maximum altitudes are shown as gray lines, see Table 1 for slope and $R^2$ values. Note that regressions are for the western flank of the range only. The western and eastern limits of the drainage divide in each swath are indicated by the horizontal black bars. Relative positions of swaths 1, 2, and 3 can be seen in Figure 1A.

59), and sedimentary rocks ($N = 54$) is $390 \pm 180$ m, $380 \pm 210$ m, $340 \pm 140$ m and $400 \pm 220$ m, respectively.

Neither the study area as a whole nor the areas in cirque basins have normally distributed slopes (Fig. 7B). The average slope over the entire study region is 19°, much lower than the 29° average slope of cirque basins. Because areas with slopes less than ~5° most likely represent valley bottoms and depositional rather than erosional terrain (e.g., Montgomery, 2001), we also calculated average slopes with this "depositional" topography excluded. Removing the areas with <5° slopes (23% of the total area and 9% of the cirque basins have slopes <5°) results in average slopes of 24° for the overall study area and 31° for the cirque basins.

Reiners et al. (2003) showed that the highest long-term average exhumation rates in the Cascades in central Washington occur in the middle of the western flank, and the exhumation rate decreases toward the far west and east sides of the range. Within our study area, the highest exhumation rates from Reiners et al. (2003) are located 30 to 40 km west of the highest peaks (Fig. 8). In addition, there is a difference in the relationship between the various erosion models and exhumation rates at specific locations in the western Cascade flank versus the eastern Cascade flank. On the west side of the crest, stream power is relatively low for a wide range of exhumation rates (0.06 to 0.33 km myr$^{-1}$) and a linear regression indicates an insignificant relationship ($R^2 < 0.01$;

Table 1
Slopes and linear regressions for maximum altitudes, glaciers, and cirques in swaths 1, 2, 3, and entire study area

| Feature | | Swath 1 | Swath 2 | Swath 3 | All |
|---|---|---|---|---|---|
| Maximum topography | Slope | $0.0093 \pm 0.0001$ | $0.0153 \pm 0.0002$ | $0.0124 \pm 0.0003$ | $0.014 \pm 0.0003$ |
| | $R^2$ | 0.86 | 0.83 | 0.69 | 0.77 |
| Glaciers | Slope | NA | $0.0135 \pm 0.0018$ | $0.0105 \pm 0.0023$ | $0.0106 \pm 0.0012$ |
| | $R^2$ | NA | 0.70 | 0.22 | 0.48 |
| Cirques | Slope | $0.0138 \pm 0.0018$ | $0.0145 \pm 0.0006$ | $0.0088 \pm 0.0008$ | $0.0131 \pm 0.0005$ |
| | $R^2$ | 0.56 | 0.72 | 0.64 | 0.69 |

Slopes, or cross-range gradients, are presented as unitless (km km$^{-1}$). All regressions are statistically significant ($P < 0.01$). Regressions on maximum topography calculated on western flank of the range only (Fig. 5).
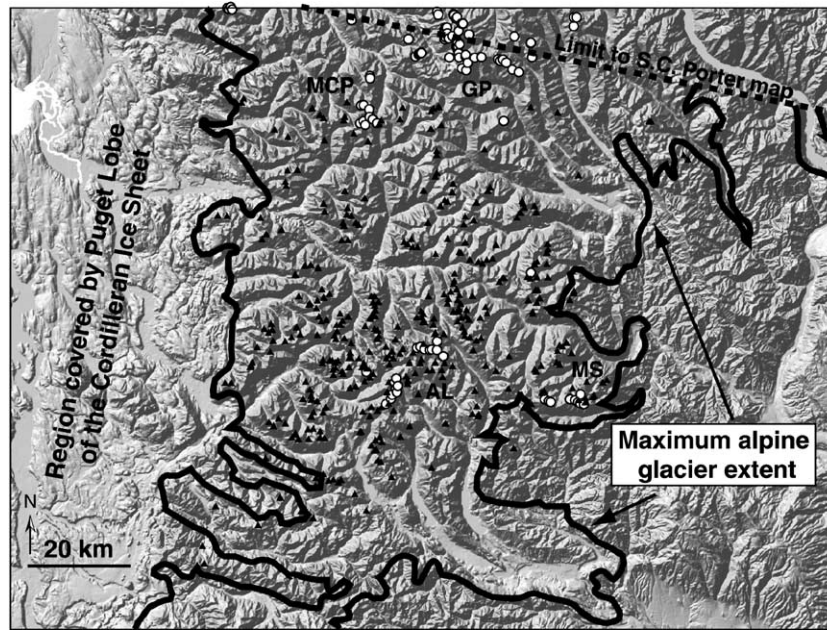
Figure 4. A. Spatial distribution of glaciers (open circles) and cirques (black triangles). Glaciers are concentrated in the areas of Glacier Peak (GP), Monte Cristo Peak (MCP), Mount Stuart (MS), and the Alpine Lakes (AL). Heavy black line shows the limit of valley glacier ice during the Quaternary maximum as mapped by S.C. Porter (unpublished data).

$P = 0.95$) (Fig. 9A, Table 2). Conversely, exhumation rates on the west flank generally increase with increasing hillslope erosion potential, defining a weak, although statistically significant relationship ($R^2 = 0.19$; $P < 0.01$) (Fig. 9B). On the east side of the range, exhumation rates increase linearly with increasing stream power ($R^2 = 0.63$, $P < 0.01$) (Fig. 9C). In contrast, the relationship between exhumation rate and hillslope erosion potential on the eastern flank is statistically insignificant ($R^2 = 0.01$; $P = 0.55$) (Fig. 9D).

## Discussion

The spatial relationship between the ELAs and the peak altitudes suggests the operation of a glacial buzzsaw, but by itself this relationship does not prove that glacial erosion limited the altitude of the range. One proposed signature of a "glacial buzzsaw" is topography that trends with the snowline despite significant variation in the rock uplift rate over the same area (e.g., Brozovic et al., 1997; Montgomery et al., 2001; Spotila et
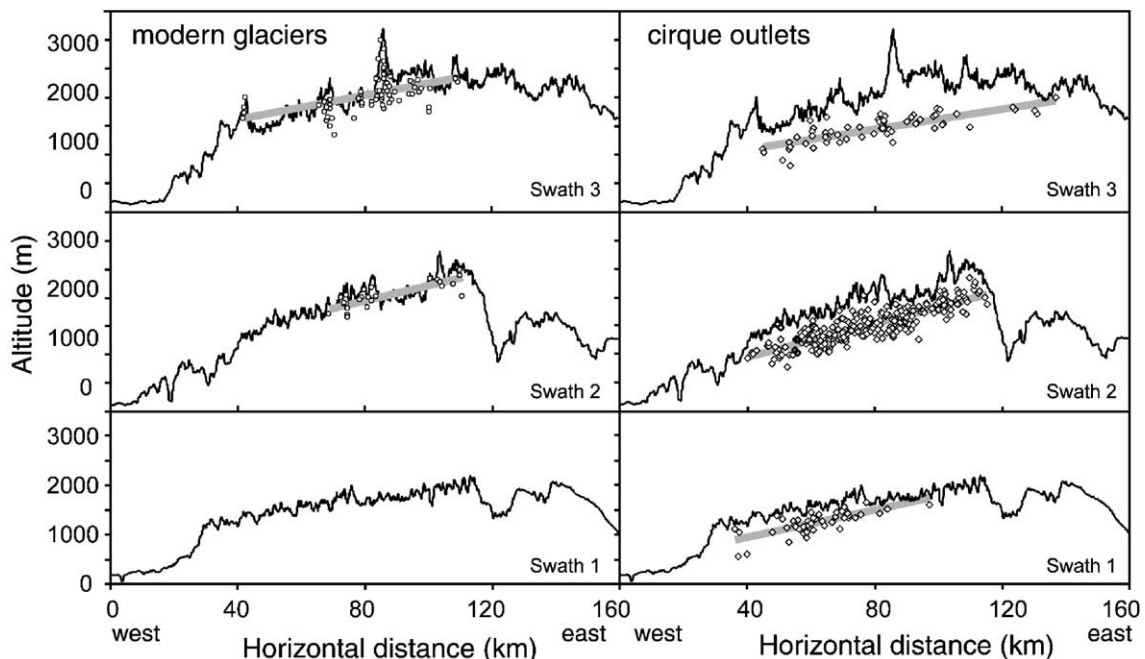


Figure 5. Cross-range trends in average glacier (left) and cirque outlet (right) altitudes shown on the three topographic subswaths. Linear least-square regressions of cirque and glacier altitudes are shown as thick gray lines; slope and $R^2$ values are in Table 1.
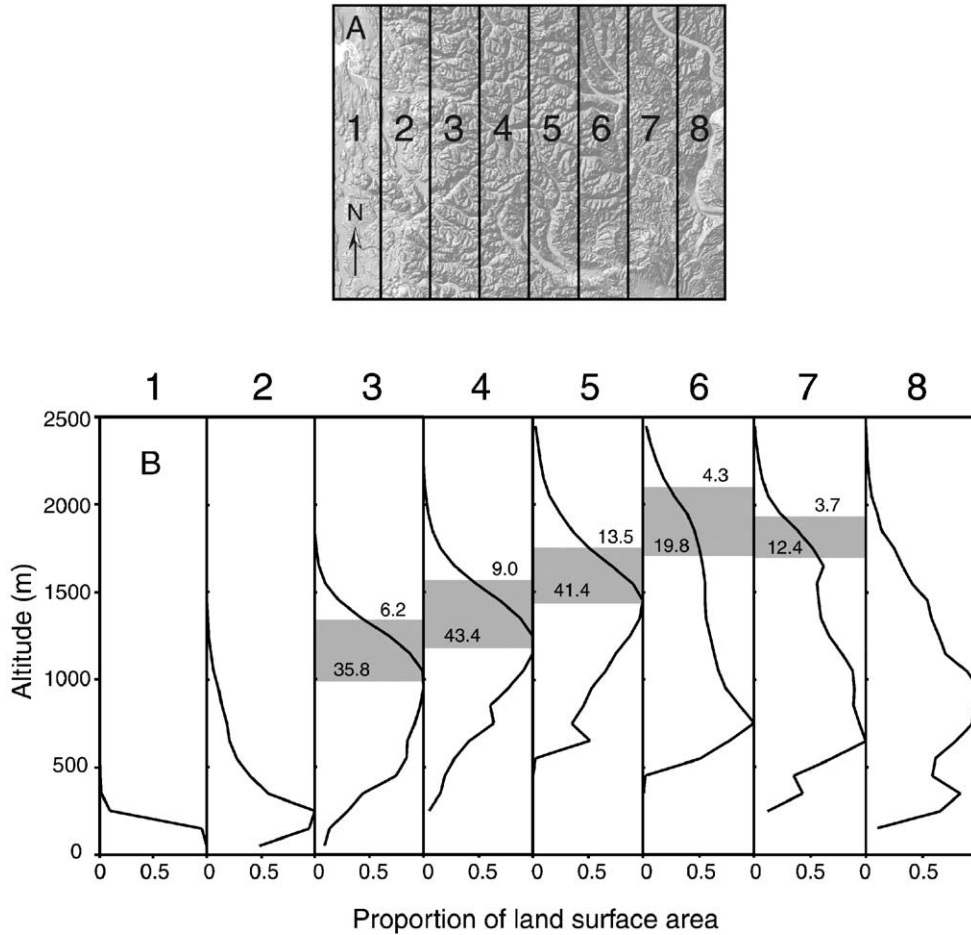
Figure 6. (A) Index map showing subdivisions for altitude–area distributions. Each subdivision is 20 km wide. (B) Normalized altitude–area distributions binned in 100 m intervals for eight subsections of study area. Distributions are shown from west to east going from left to right. The range of cirque floor altitudes within each subsection is marked with a gray box. The percentage of land area located above the lowest and highest cirques is shown for each subsection.

al., 2004). Assuming little or no change in surface elevation through time (i.e., topographic steady state), exhumation rate can be used as a proxy for rock uplift. Thus, topography that is independent of long-term exhumation but correlates with trends in the ELA suggests that glacial erosion erodes rock at rates equivalent to the rock uplift rates, regardless of how high those rates are. The ten-fold variation in exhumation rate on the west flank of the Cascades reported by Reiners et al. (2002, 2003) spans the same area where the summits define a planar "surface" that forms an envelope ≤600 m above the ELA despite substantial variation in long-term exhumation (Fig. 8). Thus, the topography of this region of the Cascades demonstrates at least one of the key components of the glacial buzzsaw.

The exhumation-rate data also allow us to demonstrate conclusively that the distinctive peak concordance on the western flank is not an erosional remnant of an uplifted peneplain, as early workers suggested (e.g., Russell, 1900). Thermochronometric data from the western flank of the Cascades indicate that long-term average exhumation rates range from 0.14 km myr$^{-1}$ to as high as 0.33 km myr$^{-1}$, corresponding to removal of ~2 to 5 vertical km of rock in the past 15 myr (Reiners et al., 2002, 2003). The summits on the west flank therefore were not once part of a

continuous topographic surface. We contend that erosion related to glaciation created the inclined topographic "surface" of the western slope of the range by shaving off high topography.

The abundance of glacial erosion features supports our hypothesis that glacial, rather than fluvial, erosion controls peak altitudes in the Cascade Range of central Washington. The widespread occurrence of cirques on the west side of the range indicates a morphologically significant "bite" out of topography above the ELA (a mode of relief reduction favored by Whipple et al., 1999). The effects of glacial erosion are also evident in the relationship between peak altitude, cirque altitude, and cirque relief. In this area, ridges and peaks rise an average of 380 ± 190 m and only rarely more than 600 m above cirque floors (Fig. 7A). Indeed, the cirque floors appear to define a general level above which the adjacent peaks and ridges extend ≤600 m higher across the study area as a whole. This height of summit altitudes above the cirques is a function of both the slope and the spacing of valleys within the topography (e.g., Schmidt and Montgomery, 1995). In the Cascades, it appears that any spatial variation in the drainage density is less important in controlling the summit altitudes than the spatial trend in the altitude of cirque floors.
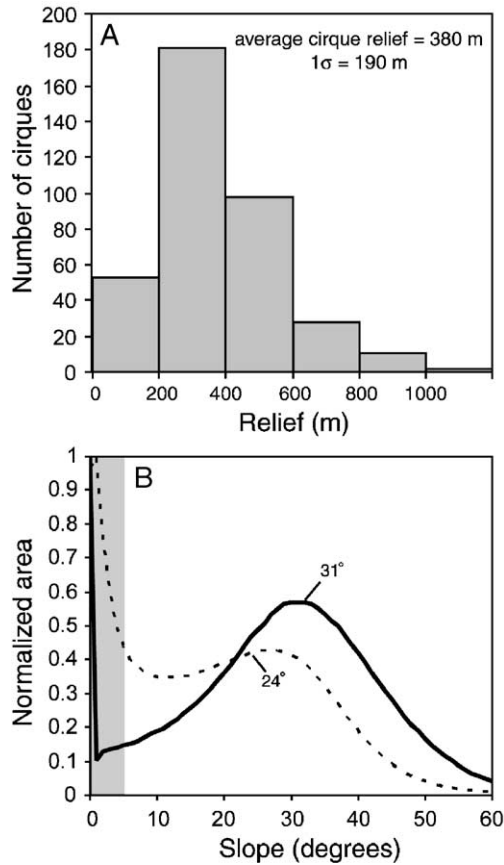
Figure 7. (A) Distribution of cirque basin relief. Total number of cirques analyzed was N = 373. Cirque relief distributions for different rock types were similar to the overall distribution, despite probable differences in rock hardness. (B) Slope distribution of entire study window (dashed line) and cirque basins only (solid line). Excluding areas with slopes <5°, which contain the majority of depositional terrain, the average slope of the entire area is 24° and the average slope of cirque basins alone is 31°.

Further evidence for the influence of glacial processes on the topography is that the lower limit of cirque altitudes is the altitude above which the relative proportion of land surface area steeply declines (Fig. 6). As in the Andes (Montgomery et al., 2001), only about 10% of the total land area lies above the zone of cirques in the central Cascades. Our area–altitude

results contrast with those of Brozovic et al. (1997), whose analysis of the Himalaya indicated a significant proportion of the land surface area lies at the modern ELA, and Meigs and Sauber (2000), who found that half or more of the land surface area in the Chugach/St. Elias Range of Alaska was located above the modern ELA. Many of the valleys in both the Himalaya and Chugach/St. Elias are full of glacier ice, and glaciers there cover a higher percentage of the topography than in the Cascades. Because the mechanical properties of glacier ice are different than rock, ice will have much different altitude–area and slope distributions than the rock of the surrounding and underlying landscape. Hence, the differences in the topographic metrics between regions may be due to the presence of extensive modern glacier ice in Alaska and the Himalaya and the lack of it in the Cascades. Modern glaciers cover <0.3% of the land surface within our study area, and the modern ELA barely intersects even the highest peaks (Fig. 5). We suggest that in the Cascades, we can define one characteristic of a "fossil" glacial buzzsaw on a landscape with few active glaciers: a steep drop off in land area above the altitude of the most erosionally significant ELA, in this case the Quaternary average ELA defined by the lower limit of the zone of cirques.

The observed lack of correlation between stream power and exhumation rates further suggests that a process other than long-term fluvial erosion governed the exhumation of the western flank of the Cascades (Fig. 9). Glacial erosion scales non-linearly with precipitation, such that higher snow accumulation rates will increase ice thickness, thus increasing basal ice velocities and therefore erosion rates (Tomkin and Braun, 2002). Glaciers may also reduce fluvial erosion downstream of glacier termini by increasing sediment loads (Whipple et al., 1999). Glacial processes acting over the past 2 to 3 myr could explain why exhumation rates near the divide on the western flank of the Cascades can be quite high where stream power is relatively low. The stronger relationship between stream power and exhumation on the eastern flank of the range suggests that fluvial erosion there has been a dominant landscape-lowering process, and that glacial erosion has removed less material on the east flank than on the west flank.
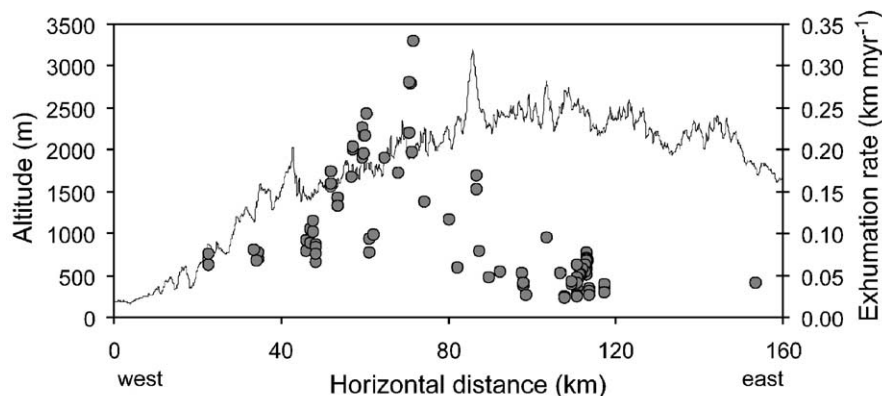


Figure 8. Cross-range maximum altitude profile showing spatial pattern of exhumation rates from apatite (U-Th)/He thermochronometry (open circles). All exhumation data are from Reiners et al. (2002, 2003). Exhumation rates are highest ~70 km east of the western edge of the study area, whereas the highest altitudes are located 30 to 40 km farther to the east. Note that the exhumation rate varies by at least an order of ten across the region of peak concordance.
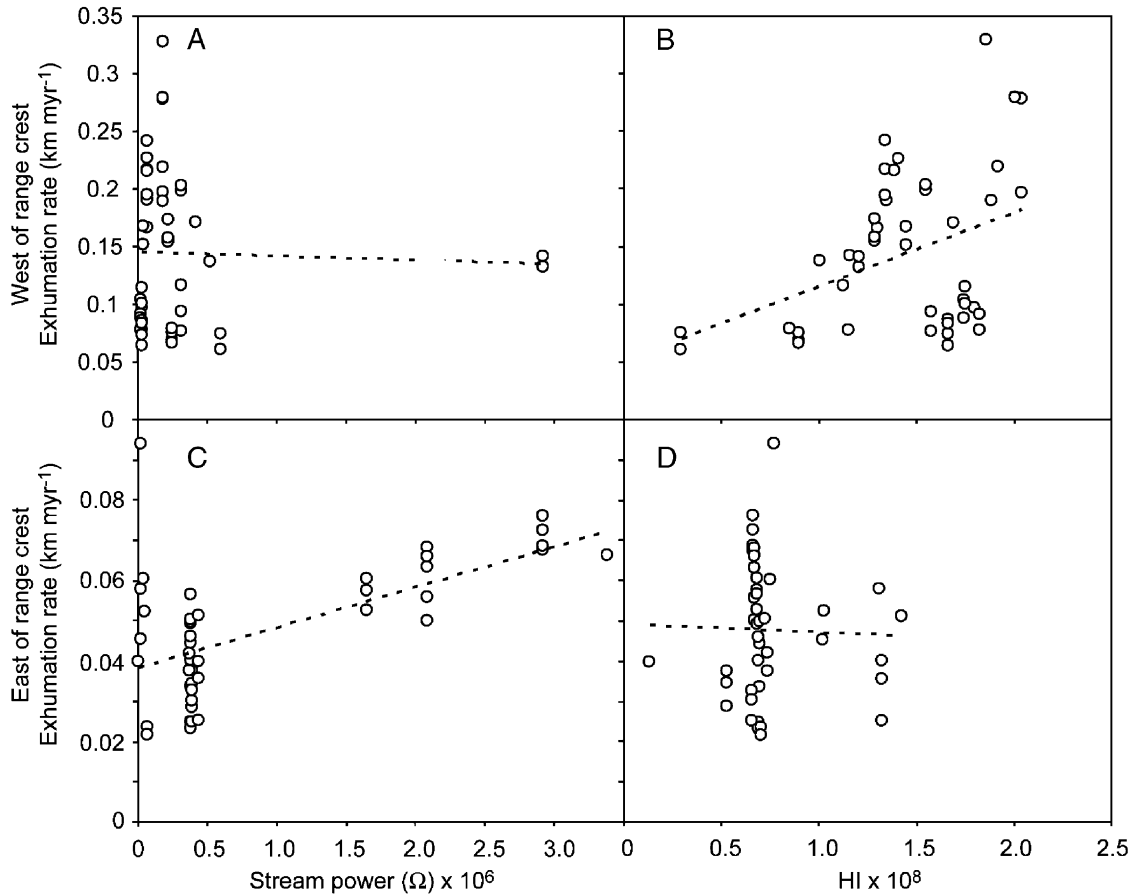
Figure 9. Relationships between erosion models and measured exhumation rates from AHe thermochronometry for sample locations east and west of the drainage divide (AHe data from Reiners et al. (2002, 2003). (A) Maximum stream-power erosion potential ($\Omega$) within a 5-km radius has no significant relationship to exhumation rate for AHe sample locations west of the range crest. Removing the outliers with high erosion potential changes the slope, but not the intercept, $R^2$ value, or significance of the linear least-squares trendline. (B) Average hillslope erosion potential (HI) within a 5-km radius increases with increasing exhumation rate for west-side samples. (C) $\Omega$ increases with increasing exhumation rate for samples located east of the range crest. (D) HI has a statistically insignificant relationship with exhumation rate for samples located east of the range crest. See Table 2 for the slope, intercept, $R^2$ and $P$ value for all linear regressions.

If the peak altitudes in the Cascades are ultimately controlled by the position of the ELA, then what specific processes are responsible for limiting the maximum altitude across the range? We propose that a combination of glacial and nonglacial erosion may link the ELA to the maximum altitude trends. First, the many cirques at and above the Quaternary average ELA provide direct evidence that glacial erosion removed a topographically significant volume of rock at high altitude. Subglacial bedrock erosion rates tend to be highest where ice flux and velocity are greatest; these conditions often occur at or near the ELA (MacGregor et al., 2000; Tomkin and Braun, 2000). Second, we suggest that the morphology created by glacial erosion—wide cirque

bottoms with steep sides—increases the potential for hillslope processes such as bedrock landslides on the steep headwalls leading up to the ridges and peaks adjacent to the cirques. It has long been noted that the high topography in the Cascades consists of glacial features such as horns and arêtes, examples of steep alpine features that form adjacent to glaciated valleys and not under the glaciers themselves. These nunataks exposed above the ice were subject to periglacial processes, such as frost heave and ice wedging, throughout the Quaternary. When the ice retreats, the deglaciated landscape becomes susceptible to paraglacial slope failure due to steepening, fracturing, and debutressing, thus resulting in higher erosion rates focused at and above the ELA (Ballantyne, 2002). The maintenance of steep topography at and above the ELA is supported by our slope analysis: the slopes surrounding cirque basins are very steep, with an average slope of 31°. In the Cascades, glacial erosion appears to create threshold hillslopes above the Quaternary average ELA, on which slight increases in slope lead to large increases in long-term erosion rate (e.g., Schmidt and Montgomery, 1995; Montgomery, 2001; Montgomery and Brandon, 2002). Thus, glacially enhanced erosion of these steepened slopes would impose a limit to how high ridges can rise above cirque floors.

Table 2
Coefficients and statistical parameters for the linear least-squares regression for the measured exhumation rates and erosion models shown in Figure 9

|  | Slope | Intercept | $R^2$ | $P$ |
|---|---|---|---|---|
| West side fluvial | $0.089 \pm 1.45 \times 10^{-8}$ | $0.137 \pm 0.0109$ | <0.01 | 0.95 |
| West side hillslope | $7.26 \pm 2.19 \times 10^{-10}$ | $0.0352 \pm 0.0320$ | 0.19 | <0.01 |
| East side fluvial | $1.23 \pm 0.154 \times 10^{-8}$ | $0.0338 \pm 0.00219$ | 0.63 | <0.01 |
| East side hillslope | $-0.66 \pm 1.09 \times 10^{-10}$ | $0.0510 \pm 0.00839$ | <0.01 | 0.55 |

West and east are defined relative to the range crest shown in Figure 2.

## Summary

We conclude that the planar trend in peak altitudes across the west flank of the Cascade Range in central Washington is most likely a function of glacial and glacially mediated erosion processes, rather than the interplay between long-term fluvial erosion and tectonic uplift or the result of incision of an uplifted plateau. Specifically, we posit that the planar zone of cirque glaciers, which according to Porter (1989) developed under "average" glacial conditions, rapidly eroded the high topography through subglacial erosion and created steep, fractured, unstable hillsides above the cirque zone. The development of this steep topography above the Quaternary average ELA and subsequent rapid erosion has resulted in peaks that rise ≤600 m above the average altitude of cirque floors. This relationship between the ELA and peak altitudes holds despite steep gradients in precipitation, exhumation rate, and fluvial erosion potential.

Although we cannot exclude the possibility that some combination of tectonics and erosional processes might result in such topography, we find compelling the weight of evidence linking the ELA, cirque altitudes, slope distributions, and relief to topographic trends in Cascade peak elevations. Moreover, the topographic evidence of a glacial buzzsaw in the west-central Washington Cascades includes several distinctive characteristics. First, the peak altitude surface is located ~600 m above the zone of cirque floors, corresponding to the mean plus 1σ distance that ridges and peaks rise above individual cirque floors. Second, the amount of topography declines sharply above the altitude of the lowest cirques, with, at most, 14% of the topography rising above the highest cirques. Third, the erosional topography above the Quaternary average ELA is at or close to threshold steepness. Finally, the discordance between fluvial erosion models and measured exhumation rates on the western flank suggest that processes other than fluvial and hillslope erosion are responsible for the topography of this flank of the range. Taken together, these observations provide persuasive evidence for the influence of a glacial buzzsaw on controlling the height and morphology of the Cascade Range of central Washington State.

## References

Amerson, B., 2005. Morphometry of fluvial and glacial valleys in central Idaho. Unpublished M.S. thesis, University of Washington, 43 p.

Bagnold, R.A., 1960. Flow resistance in sinuous or irregular channels: Part 2. a theoretical model of energy loss in curved channels. USGS Professional Paper, 122–130.

Ballantyne, C.K., 2002. Paraglacial geomorphology. Quaternary Science Reviews 21, 1935–2017.

Benn, D.I., Lehmkuhl, F., 2000. Mass balance and equilibrium-line altitudes of glaciers in high-mountain environments. Quaternary International 65/66, 15–29.

Booth, D.B., Troost, K.G., Clague, J.J., Waitt, R.B., 2004. The Cordilleran ice sheet. In: Gillespie, A.R., Porter, S.C., Atwater, B.F. (Eds.), The Quaternary period in the United States, Developments in Quaternary Science, vol. 1, pp. 17–43.

Brocklehurst, S.H., Whipple, K.X., 2002. Glacial erosion and relief production in the eastern Sierra Nevada, California. Geomorphology 42, 1–24.

Brocklehurst, S.H., Whipple, K.X., 2004. Hypsometry of glaciated landscapes. Earth Surface Processes and Landforms 29, 907–926.

Brozovic, N., Burbank, D.W., Meigs, A.J., 1997. Climatic limits on landscape development in the northwestern Himalaya. Science 276, 571–574.

Burbank, D.W., Leland, J., Fielding, E., Anderson, R.S., Brozovic, N., Reid, M.R., Duncan, C., 1996. Bedrock incision, rock uplift and threshold hillslopes in the northwestern Himalayas. Nature 379, 505–510.

Charlesworth, J.K., 1957. The Quaternary Era. Arnold, London.

Daly, R.A., 1905. The accordance of summit levels among alpine mountains; the fact and its significance. Journal of Geology, 105–125.

Finlayson, D.P., Montgomery, D.R., 2003. Modeling large-scale fluvial erosion in geographic information systems. Geomorphology 53, 147–164.

Hallet, B., Hunter, L., Bogen, L., 1996. Rates of erosion and sediment evacuation by glaciers; a review of field data and their implications. Global and Planetary Change 12, 213–235.

House, M.A., Wernicke, B.P., Farley, K.A., 1997. Dating topography of the Sierra Nevada, California, using apatite (U-Th)/He ages. Nature 396, 66–69.

James, A.L., 2003. Glacial erosion and geomorphology in the northwest Sierra Nevada, CA. Geomorphology 55, 283–303.

Long, W.A., 1951. Glacial geology of the Wenatchee–Entiat area, Washington. Northwest Science 25, 3–16.

MacGregor, K.R., Anderson, R.S., Anderson, S.P., Waddington, E.D., 2000. Numerical simulations of glacial-valley longitudinal profile evolution. Geology 28, 1031–1034.

Mackin, J.H., 1941. Glacial geology of the Snoqualmie–Cedar area, Washington. Journal of Geology 49, 449–481.

Martin, Y., 2000. Modelling hillslope evolution: linear and nonlinear transport relations. Geomorphology 34, 1–21.

Martin, Y., Church, M., 1997. Diffusion in landscape development models: on the nature of basic transport relations. Earth Surface Processes and Landforms 22, 273–279.

Meigs, A., Sauber, J., 2000. Southern Alaska as an example of the long-term consequences of mountain building under the influence of glaciers. Quaternary Science Reviews 19, 1543–1562.

Mills, J.E., 1892. Stratigraphy and succession of the rocks of the Sierra Nevada of California. Geological Society of America, 413–444.

Montgomery, D.R., 2001. Slope distributions, threshold hillslopes, and steady-state topography. American Journal of Science 301, 432–454.

Montgomery, D.R., 2002. Valley formation by fluvial and glacial erosion. Geology 30, 1047–1050.

Montgomery, D.R., Brandon, M.T., 2002. Topographic controls on erosion rates in tectonically active mountain ranges. Earth and Planetary Science Letters 201, 481–489.

Montgomery, D.R., Balco, G., Willett, S.D., 2001. Climate, tectonics, and the morphology of the Andes. Geology 29, 579–582.

Page, B.M., 1939. Multiple alpine glaciation in the Leavenworth area, Washington. Journal of Geology 47, 785–815.

Porter, S.C., 1964. Composite pleistocene snow line of Olympic mountains and cascade range, Washington. Geological Society of America Bulletin 75, 477–482.

Porter, S.C., 1976a. Pleistocene glaciation on the southern part of the North Cascade Range, Washington. Geological Society of America Bulletin 87, 61–75.

Porter, S.C., 1976b. Geomorphic evidence of post-Miocene deformation of the

eastern North Cascade Range. Geological Society of America Abstracts with Programs 8, 402–403.

Porter, S.C., 1977. Present and past glaciation threshold in the Cascade Range, Washington, U.S.A.: topographic and climatic controls, and paleoclimate implications. Journal of Glaciology 18, 101–116.

Porter, S.C., 1989. Some geological implications of average Quaternary glacial conditions. Quaternary Research 32, 245–261.

Porter, S.C., 2001. Snowline depression in the tropics during the Last Glaciation. Quaternary Science Reviews 20, 1067–1091.

Reiners, P.W., Ehlers, T.A., Garver, J.I., Mitchell, S.G., Montgomery, D.R., Vance, J.A., Nicolescu, S., 2002. Late Miocene exhumation and uplift of the Washington Cascade Range. Geology 30, 767–770.

Reiners, P.W., Ehlers, T.A., Mitchell, S.G., Montgomery, D.R., 2003. Coupled spatial variations in precipitation and long-term erosion rates across the Washington Cascades. Nature 426, 645–647.

Roe, G.H., Montgomery, D.R., Hallet, B., 2002. Effects of orographic precipitation variations on the concavity of steady-state river profiles. Geology 30, 143–146.

Roering, J.J., Kirchner, J.W., Dietrich, W.E., 1999. Evidence for nonlinear, diffusive sediment transport on hillslopes and implications for landscape morphology. Water Resources Research 35, 853–870.

Rudberg, S., 1984. Fossil glacial cirques or cirque problematica at lower levels in northern and central Sweden. Geografiska Annaler 66A, 29–39.

Russell, I.C., 1900. A preliminary paper on the geology of the Cascade Mountains in northern Washington. USGS Annual Report 20 (Pt. 2), 83–210.

Schmidt, K.M., Montgomery, D.R., 1995. Limits to relief. Science 270, 617–620.

Smith, G.O., 1903. Geology and physiography of Central Washington. USGS Professional Paper 19, 1–46.

Spotila, J.A., Buscher, J.T., Meigs, A.J., Reiners, P.W., 2004. Long-term glacial erosion of active mountain belts: example from the Chugach-St. Elias Range, Alaska. Geology 32, 501–504.

Tabor, R.W., Waitt, R.B., Frizzell Jr., V.A., Swanson, D.A., Byerly, G.R., and Bentley, R.D., 1982. Geologic map of the Wenatchee 1:100,000 quadrangle, central Washington. USGS Miscellaneous Investigations Series Map 1–1311, 26 p.

Tabor, R.W., Frizzell Jr., V.A., Waitt, R.B., Swanson, D.A., Byerly, G.R., Booth, D.B., Hetherington, M.J., Zartman, R.E., 1987. Geologic map of the Chelan 30-by 60-minute quadrangle, Washington. USGS Miscellaneous Investigations Series Map I-1661, scale 1:100,000, 29 p.

Tabor, R.W., Frizzell Jr., V.A., Booth, D.B., Waitt, R.B., Whetten, J.T., Zartman, R.E., 1993. Geologic map of the Skykomish River 30- by 60-minute quadrangle, Washington. USGS Miscellaneous Investigations Series Map I-1963, scale 1:100,000, 42 p.

Tabor, R.W., Frizzell Jr., V.A., Booth, D.B., Waitt, R.B., 2000. Geologic map of the Snoqualmie Pass 30 × 60 minute quadrangle, Washington. USGS Geologic Investigations Series Map I-2538, scale 1:100,000, 57 p.

Thompson, W.F., 1962. Cascade alp slopes and Gipfelfluren as clima-geomorphic phenomena. Erdkunde 16, 81–94.

Tomkin, J.H., Braun, J., 2002. The influence of alpine glaciation on the relief of tectonically active mountain belts. American Journal of Science 302, 169–190.

Waitt Jr., R.B., 1975. Late pleistocene alpine glaciers and the cordilleran ice sheet at Washington pass, north Cascade Range, Washington. Arctic and Alpine Research 7, 25–32.

Waitt Jr., R.B., Thorson, R.M., 1983. The Cordilleran ice sheet in Washington, Idaho and Montana. In: Porter, S.C. (Ed.), Late Quaternary Environments of the United States. University of Minnesota Press, Minneapolis, pp. 53–70.

Weissenborn, A.E., 1969. Geologic Map of Washington. USGS Miscellaneous Geologic Investigations Map I-583.

Whipple, K.X., Kirby, E., Brocklehurst, S.H., 1999. Geomorphic limits to climate-induced increases in topographic relief. Nature 401, 39–43.

Willis, B., 1903. Physiography and deformation of the Wenatchee-Chelan district Cascade Range. USGS Professional Paper 19, 47–97.